Increasing the field for application of magnesium by ultraceramic®: Corrosion and wear protection by plasma electrolytical oxidation (PEO) of Mg alloys

Anna Buling[1], Joerg Zerrer[1]

[1]ELB®, Ludwigsburg, Germany, buling@ceranod.de

Abstract

Due to its low density und relatively high strength magnesium has an increasing potential in the lightweight area. The weight saving potential by using magnesium exceeds 50% for some components, which leads to an increasing usage of Mg alloys in the field of automotive, aerospace and mechanical engineering in the last few years. But never the less it is still a niche material [1] due to its challenging anti-corrosion protection [2]. Already in use are Mg cast alloys in components like gear cases or in steering wheels [3] as well as A- and B- pillars or as inner stiffening components of doors and hatches [4]. Also, Mg plays an important part in the multi material automotive engineering [5], which can be extended by a better control of the corrosion of its alloys.

To meet the corrosion problem, which occurs using Mg alloys in the automotive industry, but also to confront wear problems, we developed a technique to form nanocrystalline PEO coatings on Mg substrates, especially on sheet Mg plates. The atomic bond of the PEO coating to the substrate leads to a high adhesion, and its nanocrystalline structure represents a highly protective surface for the Mg substrate.

Here we report on our results of different PEO coatings on sheet Mg plates, which are characterized by electrochemical analysis methods like impedance spectroscopy and potentiodynamic polarization. Furthermore, the coatings are characterized regarding their topography and its wear resistance, while varying the coating thickness for different requirements of the application.

Keywords

Magnesium alloys, PEO, electrochemical impedance, wear protection, nanoceramics

Introduction

The increasing interest for using magnesium alloys as lightweight elements in automotive applications is thwarted by their challenging corrosion protection. While the weight saving potential by substituting other materials for magnesium exceeds 50% for some components, leading to a reduction in fuel and CO_2 emission [6], there are still unsolved problems regarding the corrosion and wear protection.
Since Mg has the lowest electrode potential [7], galvanic corrosion in the atmospheric environment is a profound problem in the case of Mg alloys [8]. This problem is faced by different alloying strategies using Al [9], [10], whereas alloying with Zn for mechanical properties improvement is reported to increase the corrosion affection in comparison to Mg metal [11].
Furthermore, Mg alloy sheets exhibit poor formability at room temperature [12], so that there is a lot of effort to increase the formability by adding elements like Ca, Sn or rare earth elements [13], [14], [15].
To increase the application field of Mg alloys in the field of automotive we developed high corrosion resistant nanocrystalline PEO coatings, which can be applied to different alloys (AM50, AZ31 and E-Form®). Hereby, the thickness can be variated and adopted to the application field. Furthermore, the PEO process was optimized for the newly observed E-Form® alloy resulting in an enclosed and more wear-resistant coating.

Materials and Methods

Materials

As sheet materials three different Mg alloys were used in this study: AM50, AZ31 and E-Form®. AM50 is a Mg-Al-Mn-system, which is known to have a high ductility accompanied by good strength [16]. In the automotive area it is already used for inner lining of tailgates in the VW Lupo [17], [18] or the door inner. AZ31 consists of Mg-Al-Zn-Mn with a lower ductility but better mechanical properties at room temperature and it is one of the most widely used Mg sheet for industrial applications [19]. By adding rare earth elements and/or Calcium to AZ31 the formability can be improved and a better creep resistance can be achieved [20], [21], [22]. POSCO developed the E-Form® alloy, which is an AZ31 with additional Ca resulting in a much higher formability than commercial AZ31B [23].

The ELB ultraceramic® PEO process was carried out using a pulsed DC power source. As a counter electrode stainless steel was used, which was formed component- specific and as the electrolyte an additivated low-alkaline was used.

Our original inhouse PEO process was firstly adopted to the AM50 and AZ31 sheet materials. The coating thickness is driven by the process time and the consumed power density. Since the thinner coatings (25 and 10 µm) showed already good corrosion resistance as shown in the results section, these thicknesses were adopted to the E-Form® sheet material. With further optimization of our coating process by a guided power density we performed optimized 10 µm PEO coating on the E-Form® sheet.

Methods

All here presented electrochemical measurements were performed in a 0,1 M NaCl solution, using a three-electrode configuration, whereas an Ag/Ag-Cl reference electrode and a platin coated titanium counter electrode were used. The sample to be examined was operated as the working electrode. For performing the measurements, the impedance equipment of Ingeniuerbuero Peter Schrems (PGU10V-1A-IMP-SR) was used running by the software EcmWin.
For the first characterisation of the samples the open circuit potential (OPC) was measured for 15 minutes. Afterwards, electrochemical impedance spectral (EIS) measurements were carried out by varying the voltage with an amplitude of 10 mV around the OCP in the range from $10^{-2} - 10^{6}$ Hz. At last, a potentiodynamic polarization measurement of each sample was performed rising the potential from -1800 mV to 600 mV (against Ag/Ag-Cl) with a velocity of 1 mV/s.

The coated surfaces were characterized regarding their roughness using a laser scanning microscope (LSM, type: Keyence VK-X100 series) and the software VK analyse module. The obtained R_a and R_p values are given for every observed surface.

Some selected samples and their cross sections are examined by second electron microscopy (SEM) with the Zeiss Auriga FEG at the University of applied Sciences, Osnabrueck. All here presented SE micrographs are recorded at an excitation energy of 15 keV using the SESI detector.

As not only the corrosion protection of the PEO coatings is of high interest but also the wear protection, the coatings were probed regarding their wear behaviour using a pin on disc tribometer from Anton Paar (TRB MZKO). As a counter body a 100Cr6 ball with a diameter of 6 mm was used. The tribometer was operated in an oscillating mode (one sliding distance 2.5 mm) with a top load of 4 N and in ambient pressure and humidity conditions. The resulting wear traces were observed using the LSM for analysing the topography.

Results

Electrochemical measurements

The corrosion behaviour of the neat AM50 and AZ31 alloys is already studied in the literature [24], [25]. Electrochemical characterization showed that the die cast Al-Ag alloys, such as AM50, show less corrosion surface propagation than the AZ31 [26].

EIS measurements were carried out after 15 min immersion in a 0.1 M NaCl solution and are represented here in the Bode plots. The results for the AM50 alloy in Figure 1 indicate that the PEO coating with 25 µm coating thickness leads to the highest impedance value at the low frequency limit ($|Z|_{(0.01\,Hz)} = 1.89 * 10^{7}\ \Omega * cm^{2}$). In the case of the phase a high phase value at the high frequency limit, a broad shape of the curve and a high phase value at the mid phase range indicate a good corrosion resistance. All these points are also fulfilled in the case of the 25 µm thick coating on AM50. The thinner coating (10 µm) shows clearly lower values for $|Z|_{(0.01\,Hz)}$ and the phase shifting at high and middle frequencies. Surprisingly, the thickest coating (50 µm) shows somewhat lower values than the 25 µm coating. Taking into account the microstructure (shown in Figure 6) the picture can be cleared: The rougher structure of the

thicker coating does not lead to a better corrosion resistance but to a decrease of it due to a higher amount of plasma discharging effects during the longer coating process.
Different PEO systems on AM50 are already tested and reported in literature. *Lue et al.* performed different PEO coatings on the AM50 alloy [27]. The initial EIS measurements show somewhat lower values for $|Z|_{(0.01\ Hz)}$ than the here presented 25 µm PEO coating. Similar values were obtained by M. Grabowski in his PhD thesis, where he compared different systems on AM50 and AZ91 alloys [28] and our coating systems performed best. With the here presented 25 µm thick PEO coating on the AM50 alloy we are in a range of a PEO combined with a thick polymer coating on AZ31 as is was reported by *Srinivasan et al.* [29].

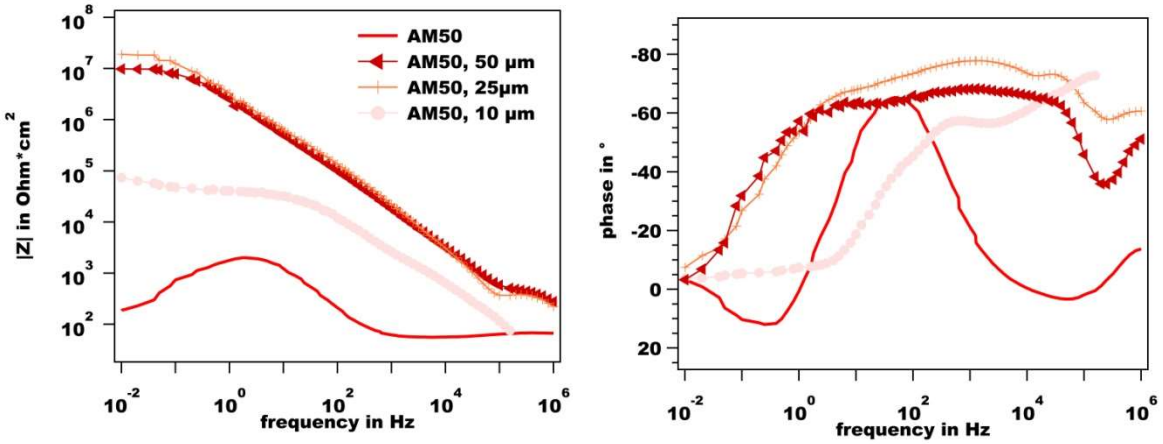

Figure 1 : EIS measurements as Bode plots for the AM50 alloy with the three different PEO coating thicknesses.

In Figure 2 the EIS results for the neat and coated AZ31 alloy are shown. For the three PEO coated samples the behaviour of the curves is very similar leading to the consumption that all three coatings result in a comparable corrosion protection in terms of self-corrosion. The 10 µm thick coating shows a somewhat slimmer shape in the phase (Figure 2b). Nonetheless, a high corrosion protection is awaited for this sample. The impedance values for all three coating systems are slightly higher compared to those reported by *Srinivasan et al.* where the coating thickness seems to be comparable as well with our 25 and 10 µm systems [30]. The 50 µm thick coating on AZ31 shows also slightly lower values than the 25 µm coating, which is in accordance to the results of the PEO coatings on the AM50 alloy discussed before.
Taking into account that the E-Form® alloy is to be seen as an optimized AZ31 alloy (by additional Ca), we decided to adapt only the thinner PEO coatings (25 and 10 µm) on that alloy, since those thicknesses seem to perform good enough in the anticorrosion behaviour and a thicker coating does not lead to a somewhat better performance.

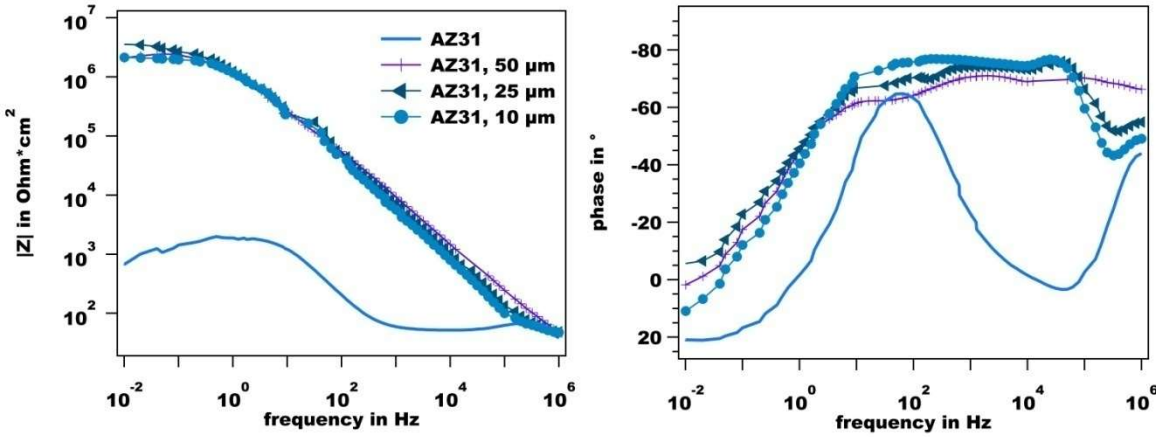

Figure 2 : EIS measurements as Bode plots for the AZ31 alloy with the three different PEO coating thicknesses

The original PEO process as it was adapted on the AZ31 alloy, was also used at the E-Form® alloy with resulting coating thicknesses of 10 and 25 µm. The EIS results are shown in Figure 3. The results for the 25 µm thick coating are comparable to those of AZ31 (Figure 2). The 10 µm coating leads to somewhat lower values in the case of the E-Form® alloy. Our optimized process (optimization by adopted current density guidance) leads to a 10 µm thick PEO coating on the E-Form® alloy with higher values for $|Z|_{(0.01\,Hz)}$, as well as for the phase value in the high and middle frequency range. Herewith, one can conclude that the optimization leads to a coating performance, which is high in terms of corrosion resistance.

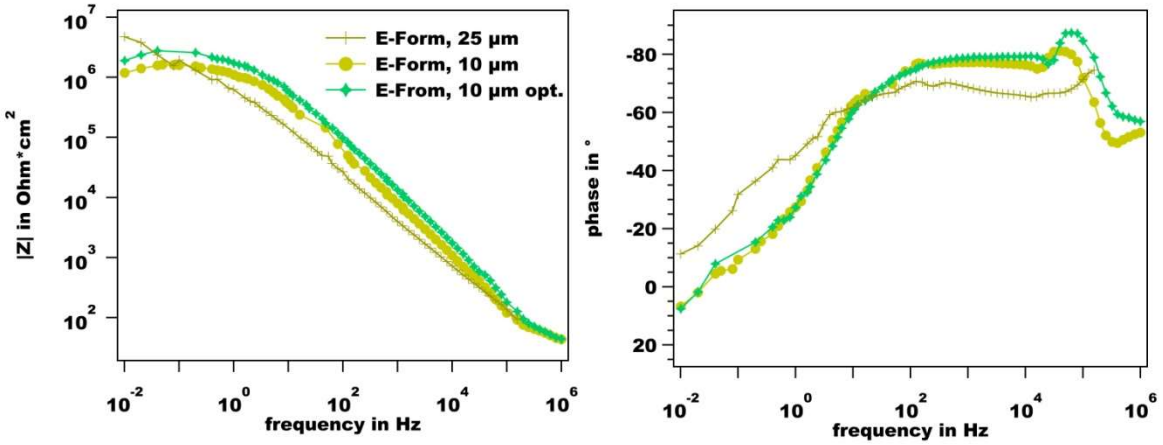

Figure 3 : EIS measurements as Bode plots for the E-Form® alloy with the two different PEO coating thicknesses in the original PEO process compared with the 10 µm thick coating of the optimized process

Potentiodynamical measurements of the PEO coated samples were performed after the EIS measurements. All results are shown in Figure 4, were the current density is presented in dependence of the voltage.

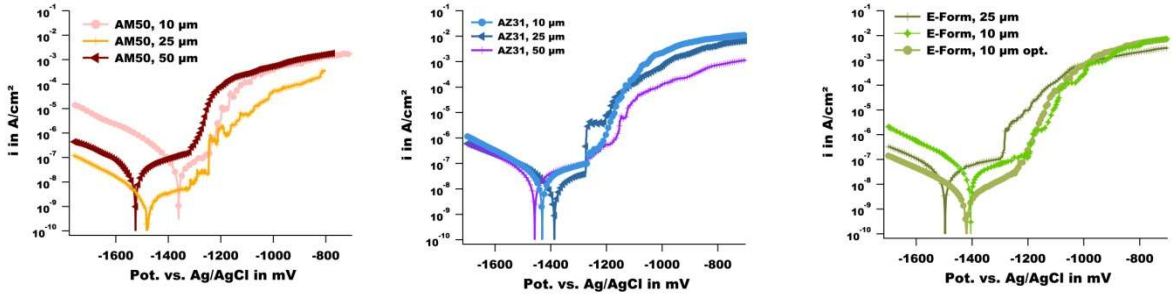

Figure 4 : Potentiodynamical measurements of the PEO coated samples

The results of the coated AM50 alloys are consistent with the previously discussed EIS results: The corrosion potential (E_{corr}) is increasing from 50 µm to 25 µm and has the highest value for the 10 µm thick coating. Furthermore, the corrosion current density (i_{corr}) (shown in Figure 5, derived from the Tafel plots in Figure 4) for the 25 µm thick coating on AM50 is 10 times lower than those of 10 µm and 50 µm thickness. Tafel plots of the AZ31 PEO coated alloy show corrosion potentials, which are shifted towards higher values. The corrosion current densities are in the same range for all three coating thicknesses, whereas the 25 µm coating shows the lowest value. In the case of the E-Form® alloy the i_{corr} value decreases with the coating thickness (from 10 µm to 25 µm) in the case of the original coating process. After the optimization of the coating process the corrosion current density decreases by an order of magnitude for the 10 µm thickness leading to a prediction of higher corrosion protection in the case of contact corrosion.

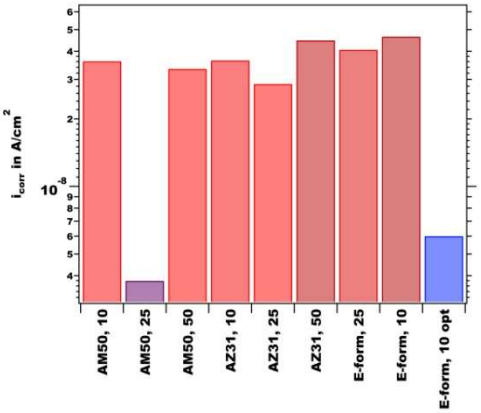

Figure 5 : Corrosion current densities for all samples, derived from the Tafel plots in Figure 4

Microstructure

Figure 6 shows the microstructure of the PEO surfaces recorded using the LSM. All micrographs were recorded using the same amplification. Obviously, in all cases for all the three alloys the topographical microstructure of the surface is getting finer by a thinner coating. This is in agreement with the process of PEO – adding the current density for longer time leads to a higher amount of discharging events on the substrate surface and, thus, to a higher roughness [31]. The optimized 10 µm coating on the Mg E-Form® sheet shown in Figure 6 i) exhibits a very fine structure.

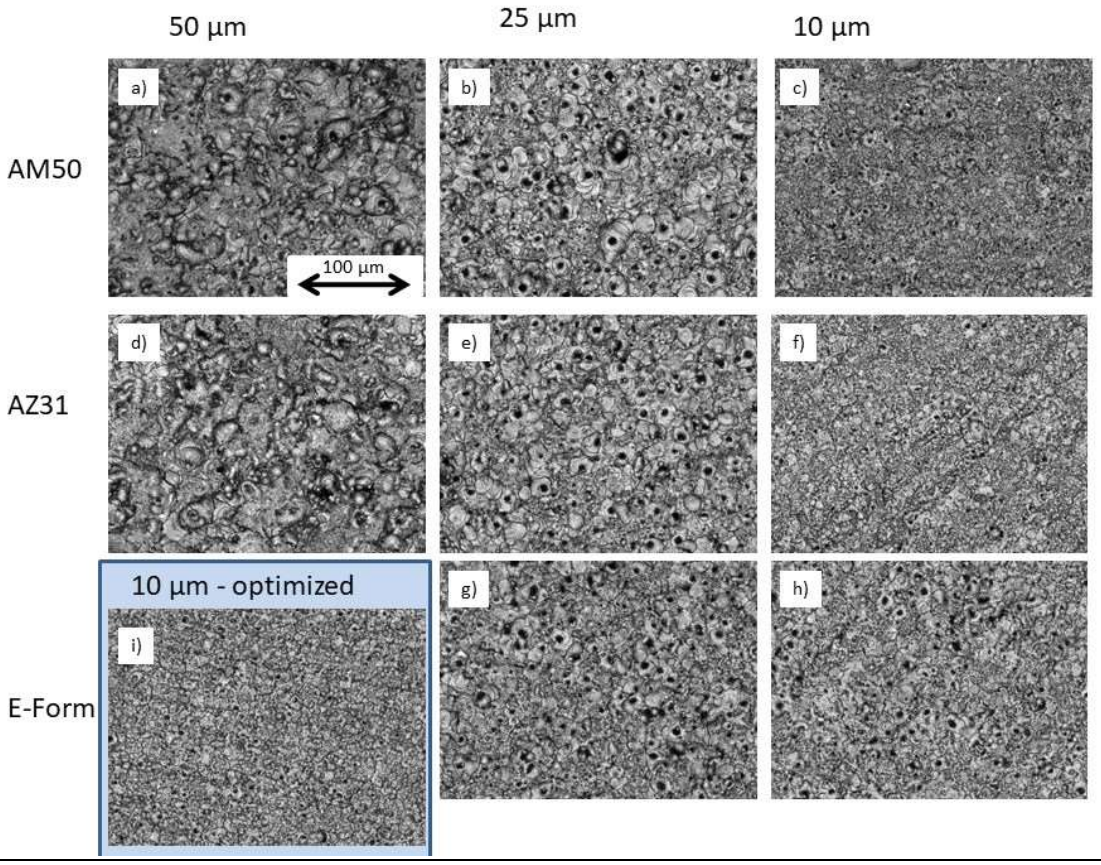

Figure 6: Surface structures of the PEO coatings detected by LSM

The roughness measurements were performed using the LSM. Here, the R_a (arithmetic mean deviation) value as well as the R_p (maximum peak perk height) are recorded using a cut off wavelength of λ_c=0.80 mm. The R_p value represents the high of peaks above the core roughness of the coating and may be a measure for the wear of the contacting body in a tribological system [32] or of the height of the coating that may be bedded in during a running-in operation [33]. Also, a high R_p value may be linked with a high coefficient of friction. As can be seen in Figure 7 for both alloys, AM50 and AZ31, the R_a and R_p values increase with increasing coating thickness. On the contrary the values slightly decrease for the E-Form® alloy with increasing coating thickness for the original coating process. Since the deviation is small, the differences in the R_a and R_p values for 10 µm and 25 µm coating thickness on the E-Form® sheet are in the range of the measurement uncertainty. The optimized coating on the E-Form® alloy shows the lowest values for R_a and R_p – here the visual impression of the micrographs in Figure 6 i) can be emphasized: The optimization of the coating process leads to a smooth surface, which exhibits a superfine microstructure.

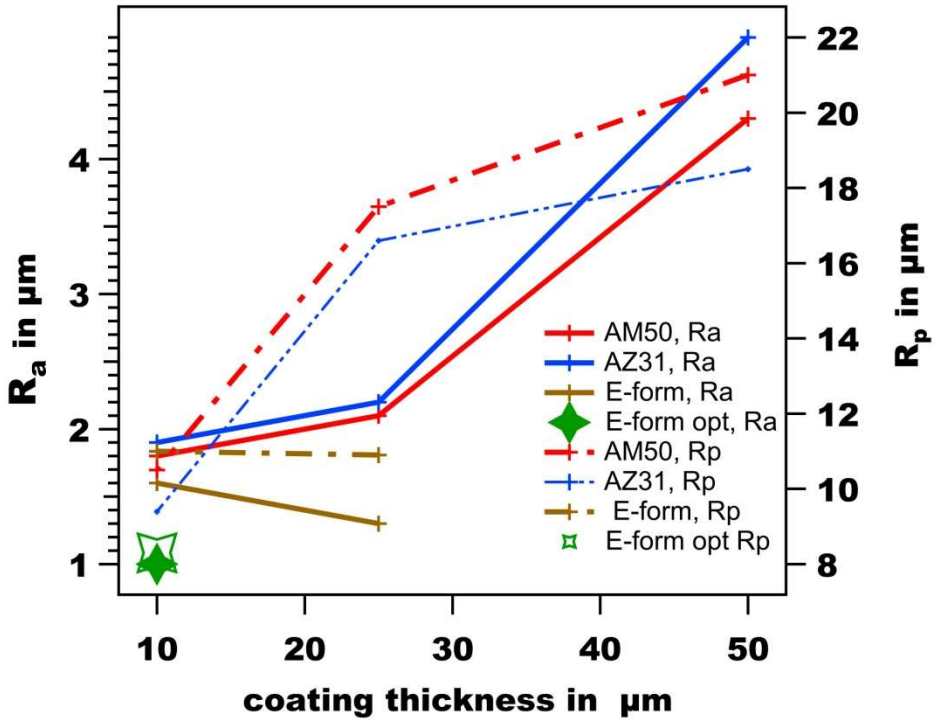

Figure 7 : Roughness measurements of the PEO coated surfaces

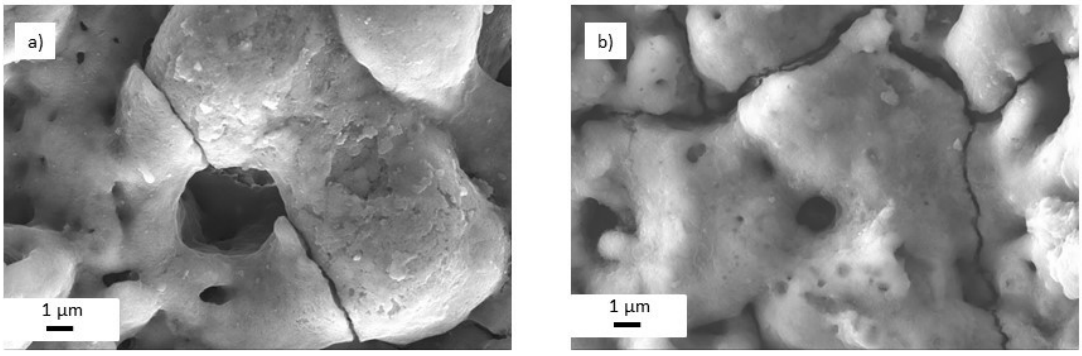

Figure 8: SEM of the pores of the PEO surfaces a) E-Form®, 10 µm PEO in original process; b) E-Form®, 10 µm PEO in optimized process

SEM micrographs of the pore structure of the PEO surfaces draw the same picture: The optimization of the PEO process on the E-Form® surface leads to a decrease of the pores by around three times compared to the same thickness coating in the original process (Figure 8).

The cross sections of the original and the optimized PEO process on the E-Form® alloy with the coating thickness of 10 µm were analysed by the SEM (Figure 9). The microstructure of the original PEO coating (Figure 9 a)) shows a compact inner layer but a porous outer layer, which leads to the higher roughness values. The optimized process (Figure 9 b)) leads to a coating, which shows some discharge channels, but almost no pores in the outer layer – the surface remains smooth in this case.

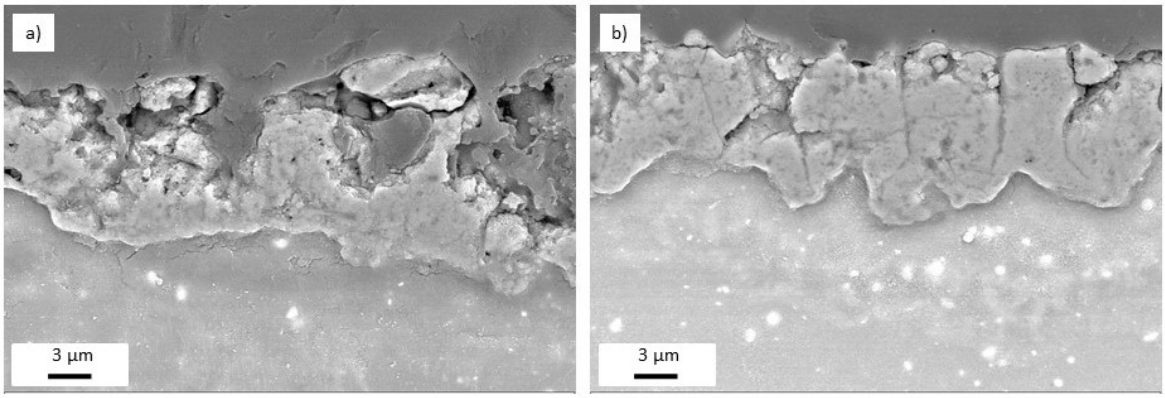

Figure 9 : SEM of cross sections a) E-Form®, 10 µm PEO in original process ; b) E-Form®, 10 µm PEO in optimized process

Wear behaviour

Pin-on-disc tests were performed on the different samples with the coating thickness of 10 and 25 µm. The coefficient of friction (COF) was monitored for a sliding distance of 80 m for all samples.
Figure 10 shows the development of the COF for all tested samples. It is obviously that in the case of the PEO coatings on AM50 and AZ31 there is no significant difference of the COF for the two tested thicknesses, which is in correlation with the R_a values for these four coating systems shown in Figure 7. In the case of the E-Form® alloy the coating with 25 µm shows a somewhat different behaviour: A decreasing of the COF is measurable around 30 m of sliding distance. After that not only an increasement but also a rising of the signal noise is visible. This leads to the assumption that there is a running-in behaviour followed by an uneven sliding. The lowest COF which is found for the 25 µm coating thickness on the AZ31 alloy is also in agreement with the lowest R_a and R_p values for that sample.

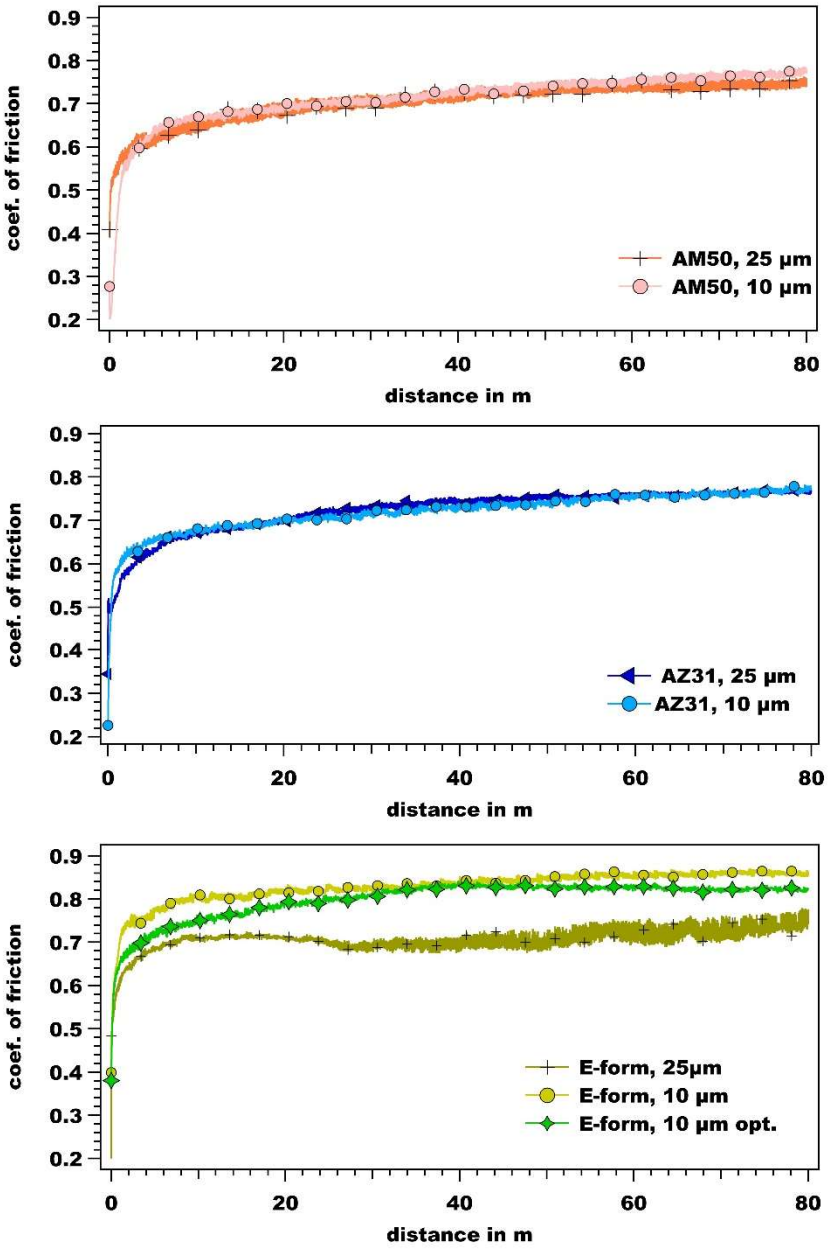

Figure 10 : coefficient of friction for the PEO coatings on the three different alloys

Figure 11 shows the average values of the COF for the tested systems, whereas the average is calculated in the quasi static area from 30 to 80 m. The shadows depict the standard deviation of the measured values. It becomes obvious that the COF values for every AM50 and AZ31 coating and the 25 µm thick PEO on the E-Form® are in the same range. Surprisingly, the 10 µm thick PEO on the E-Form® alloy leads to a much higher COF, which is not in correlation with the roughness measurements. The optimized 10 µm PEO on the E-Form® leads to a reduction of the COF but still remains clearly higher than those of AM50 and AZ31. The higher COFs for the 10 µm PEO coatings on the E-Form® alloy may be linked with Ca which is added in this alloy and might be built in in the coating, leading to a different friction behaviour at the top layer. All here measured values of COF are higher than those reported by *Ovundur et al.* for PEO coatings on 5754 Al-alloy [34].

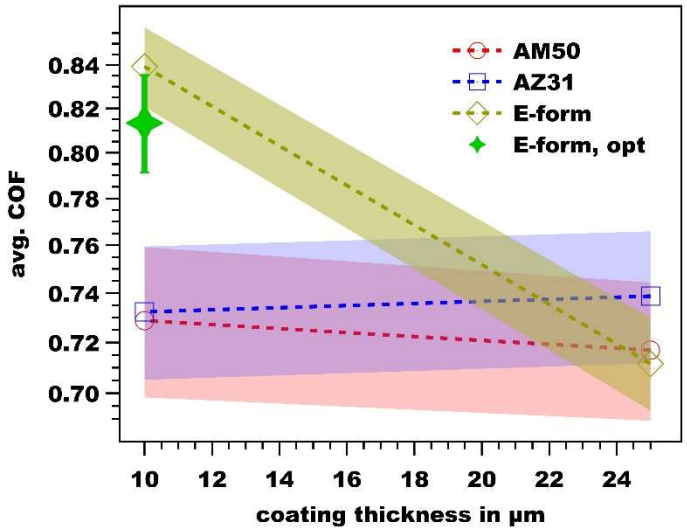

Figure 11: average COF of the wear tested PEO coatings

None of the coatings failed within the tribological testing. After a running-in behaviour characterized by an increase of the COF in the first 10 m of the testing procedure a quasi-statically state was achieved for all the here tested samples (just the 25 µm thick PEO coating on E-Form® shows a somewhat different behaviour described before).
To shed a light on the wear behaviour, LSM analysis of the tribologically tested samples was estimated. Therefore, an overlaid picture of the optical and laser-based image was recorded accompanied by the 3D-topography. The profile lines were measured orthogonal to the sliding direction. Wear results of the AM50 alloy are shown in Figure 12 : For the 25 µm thick coating only a slight smooth-out of the peaks is observable. The counter body (100Cr6 steel ball) experiences an abrasion in the running-in area. Figure 13 shows the micrograph of the steel ball for the 10 µm coating at AM50, which is exemplarily for all the other testing because the balls topography is comparable after any here presented POD testing. The thin coating of 10 µm on AM50 shows an unexpected wear behaviour: Here, wear traces appear in an angle of 45° to the sliding distance. This might be linked with the substrate topography, which plays an important role in the case of the thin coating. Nevertheless, the coating is still intact and shows no wear through down to the substrate.

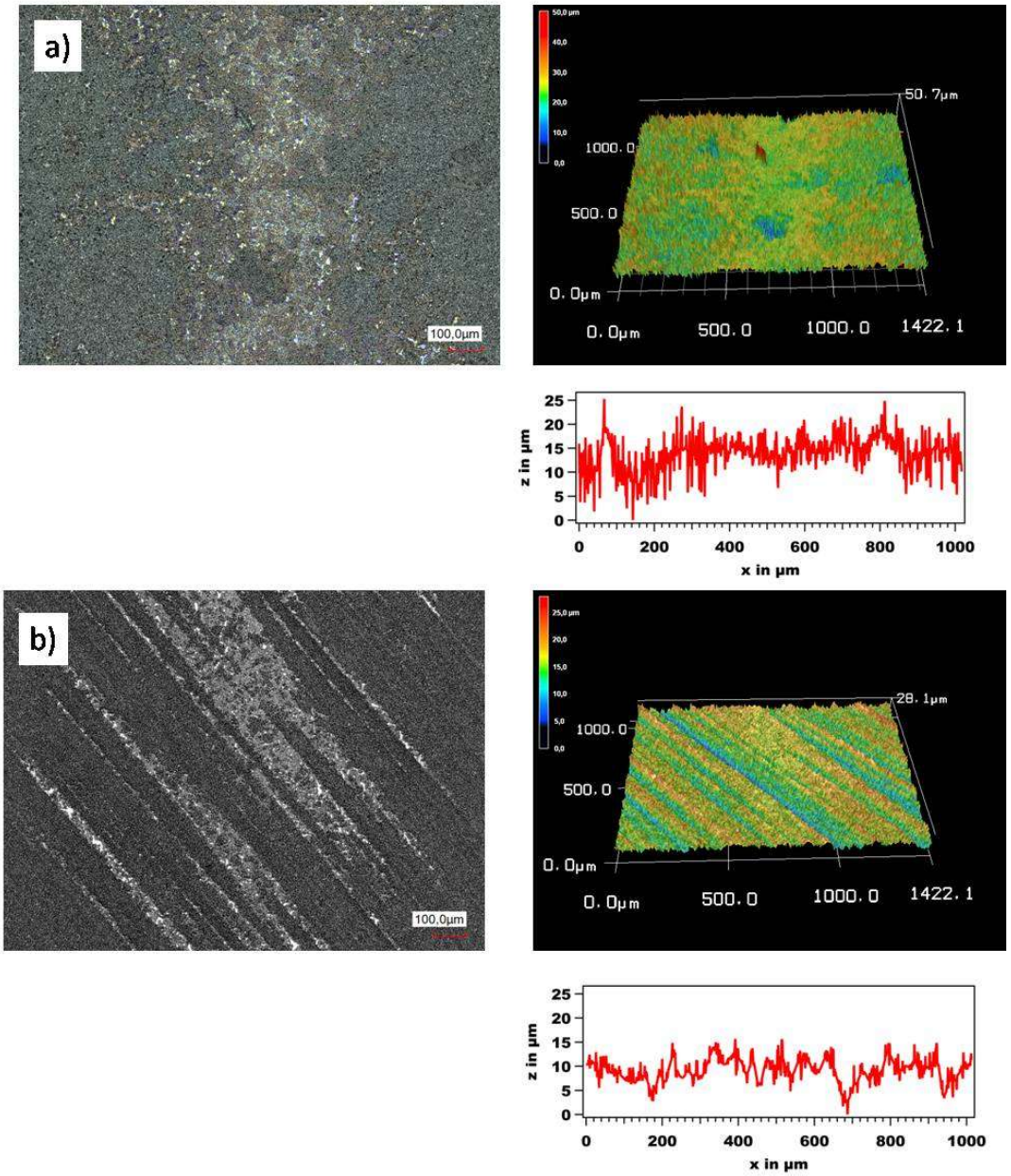

Figure 12 : LSM results after Pin-on-Disc testing of the coated AM50 alloy (the profile is always taken orthogonal to the sliding trace). a) 25 µm on AM50, b) 10 µm on AM50.

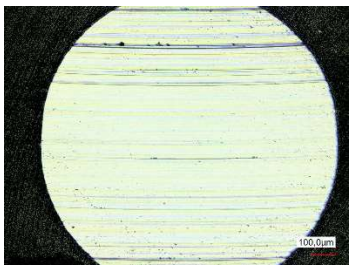

Figure 13 : LSM micrograph of the steel ball after POD testing on 10 µm PEO on AM50 alloy.

The wear results for the PEO coatings on alloy AZ31 are similar to those of AM50: The thicker coating of 25 µm shows only a grinding of the steel ball, where the debris are incorporated in the PEO coating. In the case of the thinner coating (10 µm) some slightly scratching marks are visible, while the steel debris give a structure parallel to the sliding direction.

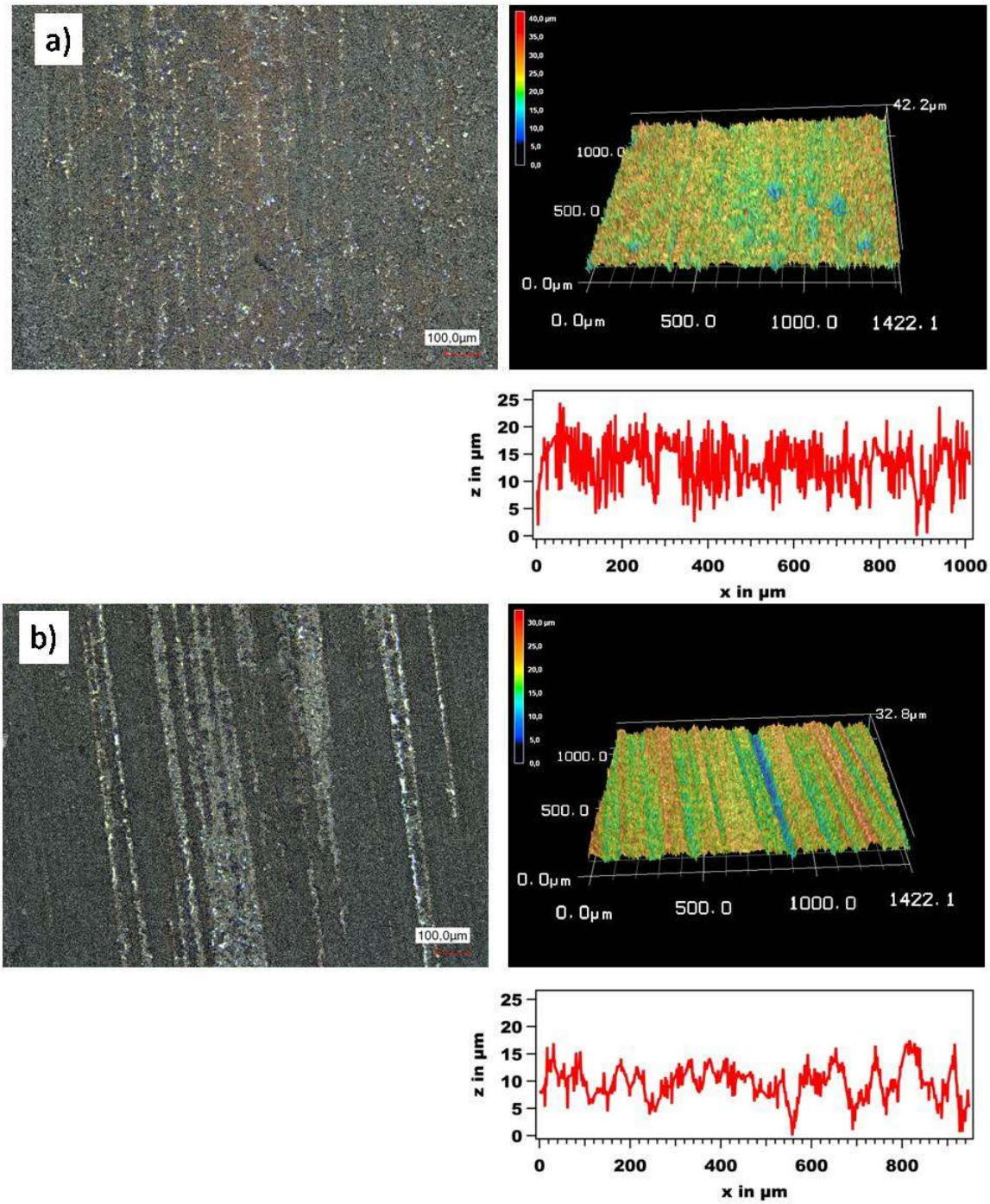

Figure 14 : LSM results after Pin-on-Disc testing of the coated AZ31 alloy (the profile is always taken orthogonal to the sliding trace). a) 25 µm on AM50, b) 10 µm on AZ31.

The most impressive wear results are obtained by the PEO coatings on the E-Form® alloy: There are only smoothing of the peaks in the coating of 10 µm. No wear marks can be detected on the coatings. In the case of the 25 µm thick coating there are no topographical changes of the coating surface, which is in agreement with the low COF in that case (see Figure 11), only the steel ball experiences a wear at the beginning of the testing phase.

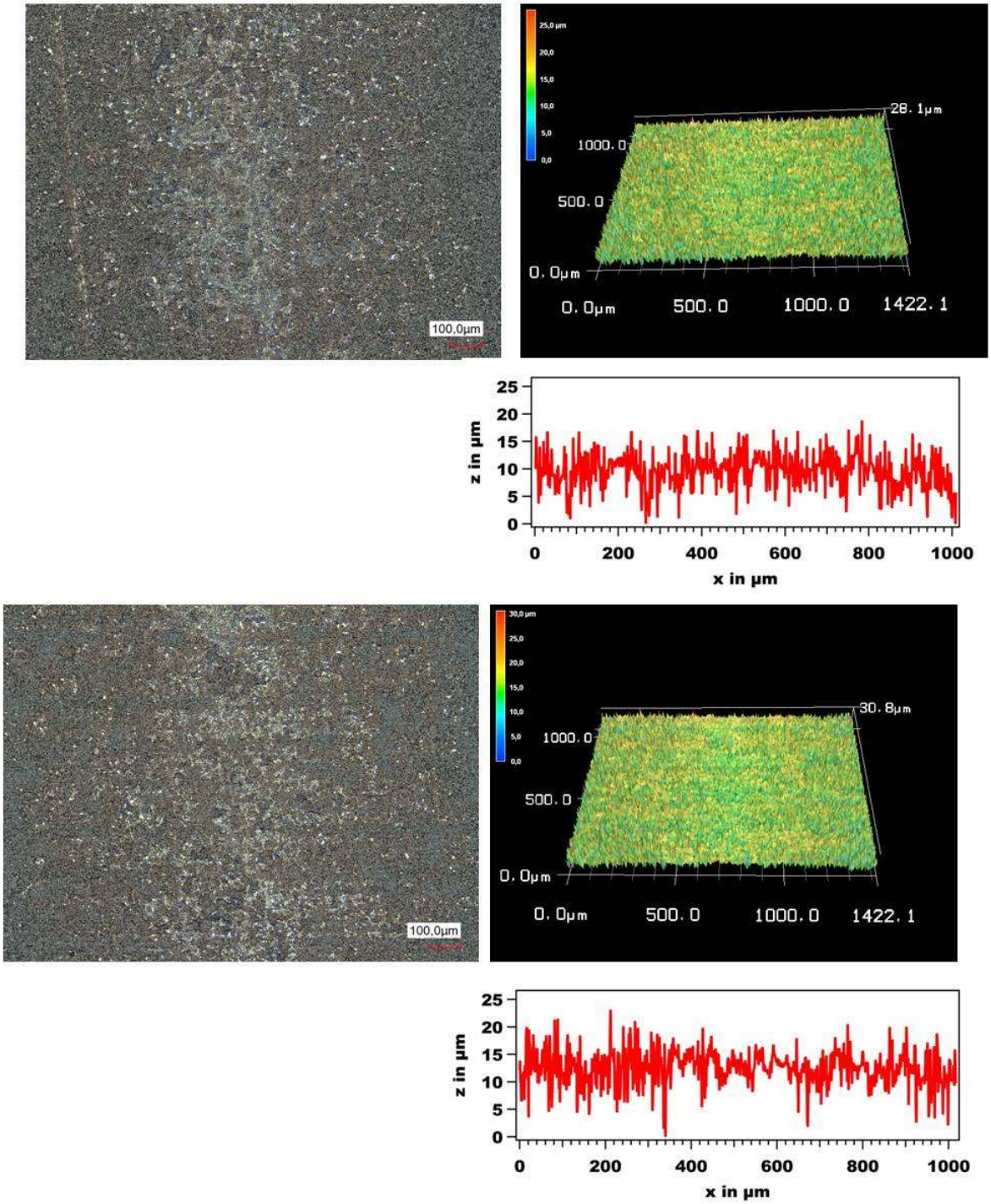

Figure 15 : LSM results after Pin-on-Disc testing of the coated E-Form® alloy (the profile is always taken orthogonal to the sliding trace). a) 25 µm on AM50, b) 10 µm on E-Form®.

The micrograph of the optimized 10 µm coating on E-Form® shows an evident trace (see Figure 16), but the 3D topography and the 2D profile show neither depth nor additional structure, leading to the assumption that the optically visible trace is due to different material reflection in this area. This might be due to the debits of the steel ball in this area.

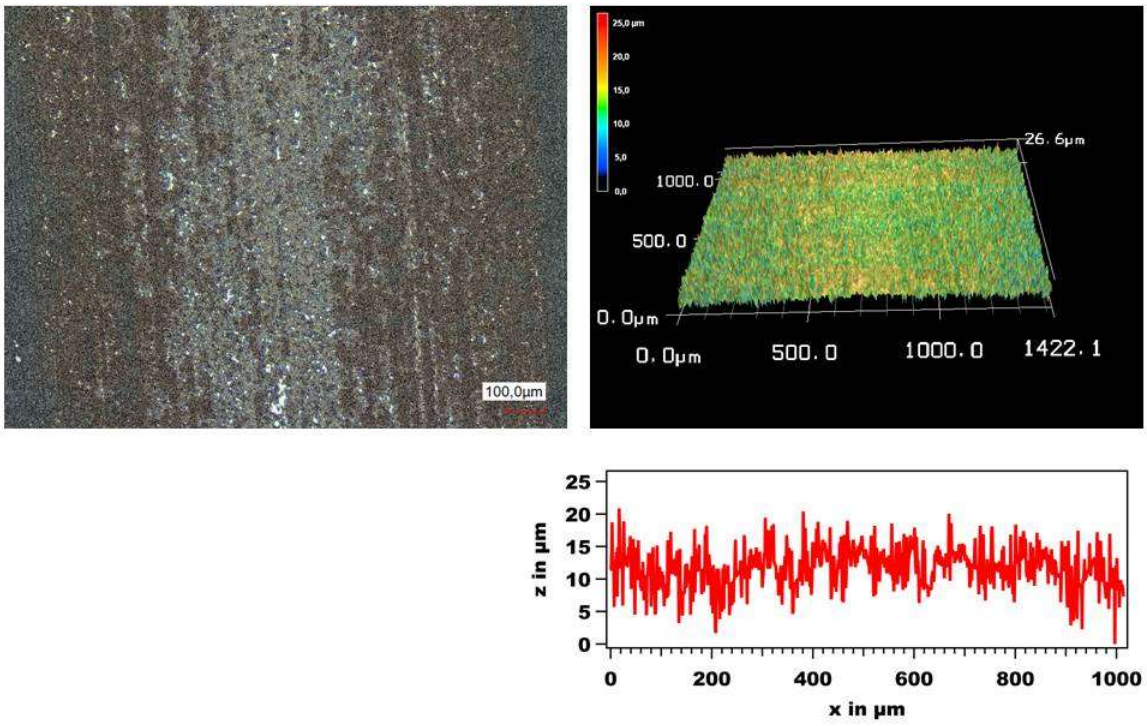

Figure 16 : LSM results after Pin-on-Disc testing of the optimized coating of 10 µm on the E-Form® alloy (the profile is always taken orthogonal to the sliding trace).

Conclusions

The here presented work investigates the corrosion and wear behavior of PEO ultraceramic® coatings on AM50, AZ31 and E-Form® alloys. The results can be concluded as followed:

- Electrochemical measurements show a high corrosion resistance for the 25 µm thick coating on the AM50 and AZ31 alloy. A further increase of the coating does not lead to an improvement. For both alloys a high corrosion protection can be achieved by 25 µm PEO coating. In the case of AZ31 a 10 µm thick coating reaches almost the same protection.
- In the case of the E-Form® alloy the 25 µm thick coating shows somewhat better performance than the 10 µm coating in our original process. After an optimization of the coating process a 10 µm nanocrystalline PEO coating could be achieved on E-Form® exhibiting the lowest corrosion current density accompanied by a low $|Z|_{0,01Hz}$ and thus having the best corrosion performance.
- Optical observations show that a thinner ultraceramic® coating leads to a finer and smoother surface structure. In the case of the 50 µm thick coatings there is always an increase of the surface roughness.
- The optimized 10 µm coating process on the E-Form® alloy leads to lowest roughness values and decreased pores on the outer layer, which is in agreement with the corrosion measurements.
- In the dry tribological testing the 10 µm and 25 µm thick coatings on AM50 and AZ31 exhibit a comparable coefficient of friction, which is also obtained by the 25 µm thick

coating on the E-Form® alloy. The 10 µm thick coating on the E-Form® alloy leads to an increased COF, which can be reduced by the optimized PEO process.

- All here examined coatings show almost no wear after the POD testing, but a wear in the terms of a grinding can be observed for every system on the steel counter body ball. Only in the case of the 10 µm thin coatings on AM50 and AZ31 there are small scratches on the coated surface without a wear trough. In the terms of wear the PEO coatings on the E-Form® alloy show the best performance. Here, the optimized 10 µm thick coating shows no wear marks at all.

The PEO ultraceramic® coatings lead to a high corrosion protection independent of the here observed Mg alloys. Already thin coatings of only 10 µm exhibit high corrosion protection, which is accompanied by high wear resistance. An optimization of the coating process on the E-Form® alloy leads to a surface, which exhibits the best wear behavior and may increase the field of applications of Mg alloys.

References

[1] A. A. Luo, "Magnesium Development as a Lightweight Material - In Competition with Other Structural Materials," in *Magnesium Technology 2017* , 2017.

[2] William J. Joost, "Reducing Vehicle Weight and Improving U.S. Energy Efficiency Using Integrated Computational Materials Engineering," *JOM,* p. 1032–1038 , 2012.

[3] Alan A. Luo, "Magnesium: Current and potential automotive applications," *JOM,* p. 42–48, 2002.

[4] P. Blanchard, G. Bretz, S. Subramanian and J. d. e. al, "The Application of Magnesium Die Casting to Vehicle Closures," *SAE International,* 2005.

[5] W. J. Joost, "Targeting High Impact R&D for Automotive Magnesium Alloys," *The Minerals, Metals & Materials Society ,* 2017.

[6] E. Aghion and D. E. B. Bronfin, "The role of the magnesium industry in protecting the environment," *Journal of Materials Processing Technology,* vol. 117, no. 3, pp. 381-385, 2001.

[7] I. Singh, M. Singh and S. Das, "A comparative corrosion behavior of Mg, AZ31 and AZ91 alloys in 3.5% NaCl solution," *Journal of Magnesium and Alloys 3,* p. 142e148, 2015.

[8] G. Song, S. Hapugoda and D. John, "Degradation of the surface appearance of magnesium and its alloys in simulated atmospheric environments," *Corrosion Science,* vol. 3, pp. 1245-1265, 2007.

[9] O. Lunder, J. E. Lein, T. K. Aune and K. Nisancioglu, "The Role of Mg17Al12 Phase in the Corrosion of Mg Alloy AZ91," *CORROSION SCIENCE,* vol. 45, no. 9, pp. 741-748, 1989.

[10] T. J. Warner, N. A. Thorne, G. Nussbaum and W. M. Stobbs, "A cross-sectional TEM study of corrosion initiation in rapidly solidified Mg-based ribbons," *Surface and Interface Analysis,* vol. 19, no. 1-12, pp. 386-392, 1992.

[11] F. -H. Cao, V. -H. Len, Z. Zhang and J. -Q. Zhang, "Corrosion behavior of magnesium and its alloy in NaCl solution," *Russian Journal of Electrochemistry,* vol. 43, no. 7, p. 837–843, 2007.

[12] J. Singh, M.-S. Kim, S.-E. Lee, E.-Y. Kim, J.-H. Kang, J.-H. Park, J.-J. Kim and S.-H. Choia, "Heterogeneity in deformation and twinning behaviors through the thickness direction in E-form Mg alloy sheets during an Erichsen test," *Materials Science and Engineering: A,* vol. 792, pp. 370-384, 2018.

[13] S.-J. Kim, Y.-S. Lee and D. Kim, "Analysis of formability of Ca-added magnesium alloy sheets at low temperatures," *Materials Characterization,* no. 113, pp. 152-159, 2016.

[14] H. Ding, X. Shi, Y. Wang, G. Cheng and S. Kamado, "Texture weakening and ductility variation of Mg–2Zn alloy with CA or RE addition," *Materials Science and Engineering: A,* no. 645, pp. 196-204, 2015.

[15] J. H. K. J. H. B. J. H. H. M.-S. S. N. J. K. Byeong-Chan Suh, "Effect of Sn addition on the microstructure and deformation behavior of Mg-3Al alloy," *Acta Materialia,* no. 124, pp. 268-279, 2017.

[16] M. K. Kulekci, "Magnesium and its alloys applications," *Int J Adv Manuf Technol,* no. 39, p. 851–865, 2008.

[17] H. Schreckenberger, "Korrosion und Korrosionsschutz von Magnesiumwerkstoffen für den Automobilbau – Korrosion und Korrosionsschutz von Magnesiumwerkstoffen für den Automobilbau – Problematik der Kontaktkorrosion," *Fortschr.-Ber. VDI Reihe,* vol. 5, 2001.

[18] C. Blawert, N. Hort and K. Kainer, "AUTOMOTIVE APPLICATIONS OF MAGNESIUM AND ITS ALLOYS," *Trans. Indian Inst. Met.,* vol. 57, pp. 397-408, 2004.

[19] J. S. Suh, Improvement in Cold Formability of AZ31 Magnesium Alloy Sheets Processed by Equal Channel Angular Pressing (ECAP), TU München, 2015.

[20] N.Stanford and M.R.Barnett, "The origin of "rare earth" texture development in extruded Mg-based alloys and its effect on tensile ductility," *Materials Science and Engineering: A,* vol. 496, no. 1-2, pp. 399-408, 2008.

[21] S.Gunabalan and D. R. Elansezhian, "Effects of Calcium Addition on Properties of Mg Alloys: A Review," in *IEEE - International Conference on Research and Development Prospects on Engineering and Technology*, 2013.

[22] D. Orlov, V. Joshi, K. N. Solanki and N. R. Neelameggham, Magnesium Technology 2018, 2018.

[23] J. Park, "Production and Applications of high formable E-form Mg alloy in POSCO," in *Magnesium Technology 2017* , San Diego, CA, 2017.

[24] I. Singh, M.Singh and S.Das, "A comparative corrosion behavior of Mg, AZ31 and AZ91 alloys in 3.5% NaCl solution," *Journal of Magnesium and Alloys,* vol. 3, no. 2, pp. 142-148, 2015.

[25] M. Grabowski and S. Virtanen, "Cathodic Corrosion of Magnesium Alloy AM50 in Deicing Salt Solutions During "Cathodic Protection"," *CORROSION,* vol. 73, no. 5, pp. 563-582., 2017.

[26] L. G. Bland, L. Scully and J. Scully, "Assessing the Corrosion of Multi-Phase Mg-Al Alloys with High Al Content by Electrochemical Impedance, Mass Loss, Hydrogen Collection, and Inductively Coupled Plasma Optical Emission Spectrometry Solution Analysis," *CURRENT TRENDS IN MG CORROSION RESEARCH,* 2017.

[27] X. Lu, S. P. Sah, N. Scharnagl, M. Störmer, M. Starykevich, M. Mohedano, C. Blawert, M. Zheludkevich and K. Kainer, "Degradation behavior of PEO coating on AM50

magnesium alloy produced from electrolytes with clay particle addition," *Surface and Coatings Technology,* vol. 269, pp. 155-169, 2015.

[28] M. Grabowski, Leichtbau mit Magnesiumlegierungen im Automobilbau: Charakterisierung der korrosiven Belastung durch Streusalzkomponenten und Auslegung des Korrosionsschutzes, Erlangen: FAU University Press, 2016.

[29] P. B. Srinivasan, N. Scharnagl, C. Blawert and W. Dietzel, "Enhanced corrosion protection of AZ31 magnesium alloy by duplex plasma electrolytic oxidation and polymer coatings," *Surface Engineering,* vol. 5, pp. 354-360, 2010.

[30] P. Srinivasan, N. Scharnagl, C. Blawert and W. Dietzel, "Enhanced corrosion protection of AZ31 magnesium alloy by duplex plasma electrolytic oxidation and polymer coatings," *Surface Engineering,* pp. 354-360, 2013.

[31] Y. Savguira, T. H. North and S. J. Thorpe, "Plasma Electrolytic Oxidation Coating of Dissimilar AZ31/AZ80 Friction Stir Welds," *Journal of The Electrochemical Society,* vol. 165, no. 2, pp. C11-C18, 2018.

[32] T. Huben and J. Becker, "Kohlenstoffbasierte Beschichtungen für automotive-Komponenten," *ViP,* no. 2, pp. 6-13, 2012.

[33] "Michigan Metrology, LLC," [Online]. Available: www.michmet.com. [Accessed 08 03 2018].

[34] M. Ovundur, F. Muhaffel and H. Cimenoglu, "Characterization and Tribological Properties of Hard Anodized and Micro Arc Oxidized 5754 Quality Aluminum Alloy," *Tribology in Industry,* vol. 1, pp. 55-59, 2015.